TITOLO THE AFRODITE BOOSTER

NOME P. Patteri, F. Tazzioli

The booster ring for the AFRODITE injector chain has been studied to achieve a low emittance ($\epsilon = 1 \cdot 10^{-7}\, m \cdot rad$ @ $1.50\, GeV$) accepting an injected beam from a positron linac without an intermediate positron accumulator.

The lattice has been designed using the same magnetic elements of the main ring, bearing in mind that substantial cost reduction can be obtained with this approach.The booster final energy can be easily raised to $2.00\, GeV$, if required by AFRODITE upgrading, because field gradients are lower than in the main ring.

The beam losses in the first stage of acceleration, before the injected beam is shrinked by damping, have been estimated and no significant efficiency reduction is foreseen after closed orbit correction.

The filling time, both in single bunch mode and multibunch mode, depends mainly on the achievable positron current from the linac.

THE LATTICE

The booster ring is basically a FODO structure with two long insertions matched to the FODO arcs; the insertions provide two long dispersion free straight sections for injection and estraction devices and four smaller sections. The magnetic structure is composed of 24 bending magnets, each $1.31\, m$ long with a radius of curvature $\rho = 5.00\, m$ and a field $B = 1.00\, Tesla @ 1.5\, GeV$, and of 38 quadrupoles, $.40\, m$ long and with a maximum gradient of $10.2\, Tesla/m$. In the matching sections between FODO arc and dispersion free section enough room results to house RF cavity and to put kickers and bumpers at the right phase displacement from deflectors. In fig. 1 the optical functions β_x, β_z and η are shown along 1/4 machine. In tab. 1 a summary of booster parameters is given. In tab. 2 the values of the optical functions are tabulated at the end of each element of the lattice from the middle of the insertion to the end of the first FODO cell in the arc. The magnetic element strenghts are also given.

Cromaticity correction has been obtained using two families of sextupoles, inserting a couple of SF and SD in each FODO cell. Q-shift with amplitude is corrected by one family of sextupoles SH1 at the ends of the straight sections. The sextupole parameters are summarized in tab. 3. The plots of Q_x and Q_z vs momentum error and the optical function relative variations vs momentum error are shown in figs. 3,4 and 5. In fig.6 limits of dynamic aperture are shown for on-energy particles and for particles with momentum error $\Delta E = 20\sigma_p$ i.e. $\Delta E/E \approx 1.2\%$.

INJECTION

A single turn, single shot injection scheme has been considered. In fig. 2 details of the long straight sections are given, showing the position and the phase displacement of the injection/extraction devices. The beam from linac leaves the injection deflector parallel to the orbit in a high β section and is put on the reference orbit by a kicker located

$\pi/2$ downstream. Owing to the absence of residual oscillation around the reference orbit, the booster acceptance is set only by linac emittance. Assuming the linac parameters $\epsilon_J = 1 \cdot 10^{-5}\, m \cdot rad$ and $\sigma_E/E = 1.\%$ at injection the maximum beam size $\sigma_x = 19.4\, mm$ is in the focusing quadrupoles of FODO arcs; an elliptical pipe housed in a quadrupole bore with radius $30\, mm$ contains $\approx 2\sigma_x$, which assures a nearly unit injection efficiency.

Beam enlargement due to increased energy spread in synchrotron motion has to be avoided injecting at the center of the RF bucket. Assuming $RF_{booster} = 50\, MHz$ a positron pulse lenght less than $10\, ns$ is required.

At injection energy $E_J = 250\, MeV$ the deflector requirements are not severe (e.g. $L_{SJ} = 1.5\, m$, $B_{SJ} = .10\, Tesla$) and can be easily modified to optimize the linac to booster transport channel.

The strenght of the kicker KJ is determined by the distance δx_{KJ} between the reference orbit and the center of the injected beam; assuming for the beam width at injection $\sigma_x = 11.6\, mm$, as would result by a gaussian phase space distribution, and taking a septum thickness $s = 3\, mm$ with its internal side $20\, mm$ far apart from the orbit,to allow $\approx 2\sigma_x$ for the injected beam, we get $\delta x_{KJ} = 34.6\, mm$. The kicker deflecting angle $(B \cdot L)_{KJ} = 7.7\, mrad$ can be obtained by a pulsed magnet with $L_{KJ} = .5\, m$ and $B_{KJ} = 1.28 \cdot 10^{-2}\, Tesla$. If only single bunch injection is foreseen, a fall time $\approx 150\, ns$ is acceptable; in multibunch mode much shorter fall time is required.

EXTRACTION

Single turn extraction will be accomplished by means of a slow bumper magnet (called BUMPER 1 or BUMPER 2 in fig. 6) to move the beam near the extraction septum, and a fast kicker to deflect the bunch into the septum.

Extraction devices are to be dimensioned for $2\, GeV$ operation.

The internal side of the septum is $20\, mm$ far from the orbit, to have the same aperture as at the location of the injection septum. A closed orbit distortion $\delta x = 20\, mm$ can be obtained by bumper B1, $.5\, m$ long with a field $B_{B1} = 2.54 \cdot 10^{-2}\, Tesla$, or by bumper B2 using the bending magnet with an additional coil allowing a field variation of $1.25 \cdot 10^{-2}\, Tesla$; of course these are upper limit values, because the closed orbit has to be kept a few millimeters apart from the septum to avoid beam loss before extraction.

The deflection produced by the extraction kicker must be equal to the beam width plus the septum thickness s; assuming $s = 5\, mm$ and $4 + 2\sigma_x$ clearance on internal and external side of the septum results $\delta x_{KE} \approx 14\, mm$; it can be obtained by the extraction kicker KE, $1.0\, m$ long with a field $B_{KE} = 2.08 \cdot 10^{-2}\, Tesla$.

A single extraction septum with $L_{SE} = 2.0\, m$ and $B_{SE} = .219\, Tesla$ asimmetrically placed in the extraction section, will produce a displacement $\delta x_E = 25\, cm$ of the extracted beam at the location of the downstream quadrupole, allowing enough room for the extraction channel.

REPETITION RATE AND FILLING TIME

The upper limit to repetition rate is imposed by betatron damping time $\tau_{betatron} = 8.8\, ms\, @\, 1.5\, GeV$; a flat top longer than 2τ is required to assure that the final emittance is settled; taking into account the raise and fall time in the acceleration cycle and a quiescent period, a $10\,Hz$ repetition rate is reasonable. Although more detailed studies have to be done when designing the power supply system, no major improvement is aspected.

With a $20\,mA$, $10\,ns$ current pulse at $10\,Hz$ repetition rate an injecting rate of $2.2\,mA/s$ in AFRODITE could be obtained if 100 % efficiency is assumed.

As it has been seen, a radial clearance equal to $\approx 2\sigma_x$ is given in critical point at injection and extraction.

Energy oscillations of the injected beam are to be considered more carefully; a $10\,ns$ pulse is too long to be comprised in the $50\,MHz$ RF bucket without increase in energy spread; a partial loss of the injected beam should be taken into account due to this effect, but it should be considered also that σ_x has been computed by a pessimistic linear combination of the σ due to emittance and to energy spread, which are nearly equal, while a quadratic one could be used, resulting a larger allowance for the beam. A better estimation should also take into account pulse shape and real energy distribution.

If the efficiency factor is 25 %, as it is customarily assumed, a filling rate of $.55\,mA/s$ is obtained.

TABLE 1

Energy	1500	MeV
Emittance	$9.5 \cdot 10^{-8}$	$m \cdot rad$
Lenght	79.060	m
Q_x	5.117	
Q_z	2.844	
Q'_x	-7.0	
Q'_z	-5.0	
α_C	$4.1 \cdot 10^{-2}$	
σ_P	$5.8 \cdot 10^{-4}$	
$\Delta E/turn$	90	keV
$\nu_{revolution}$	3.7920	MHz
$\tau_{betatron}$	8.8	ms
$\tau_{synchrotron}$	4.4	ms
Superperiodicity	2	
FODO cell/superperiod	5	
straight section lenght	5.00	m
magnet	24	
curvature radius	5	m
B_{max} @ 1.5 GeV	1.0	*Tesla*
quadrupoles, q. families	38, 5	
$dB/dx\|_{max}$	10.2	*Tesla/m*

TABLE 2

see following page

TABLE 3

sextupole	*no.*	$K2$ (m^{-2})	*Gradient* (T/m^2 per $L = .2\,m$)
SF	12	-1.272	31.8
SD	12	2.601	65.0
$SH1$	4	$-.405$	1.1

N	EL	BETAX	BETAZ	PSI	PSI'	MUX	MUZ
0	0	13.5258	4.6199	.0000	0.0000	0.0000	0.0000
1	1	13.9878	5.9728	.0000	0.0000	.1828	.4960
2	2	10.9089	8.1404	.0000	-.0000	.2138	.5558
3	1	6.4905	12.2545	.0000	-.0000	.2550	.5905
4	3	3.8938	14.3867	.0000	-.0000	.3380	.6194
5	1	2.4109	12.4580	.0000	-.0000	.5347	.6641
6	5	2.4109	12.4580	.0000	-.0000	.5347	.6641
7	4	1.2223	8.2041	.1706	.2590	1.3895	.7941
8	5	1.2223	8.2041	.1706	.2635	1.3895	.7941
9	1	3.2345	4.4124	.5598	.2635	2.2268	1.0421
10	3	4.6994	3.4283	.6875	.3790	2.3308	1.1438
11	1	8.0838	2.0562	.9084	.3790	2.4255	1.3652
12	2	8.0781	2.0564	.9084	-.3790	2.4724	1.5719
13	1	6.2023	2.6868	.7948	-.3790	2.5148	1.6999
14	5	6.2023	2.6868	.7948	-.3580	2.5148	1.6999
15	4	1.2365	7.0378	.4746	-.1280	3.0015	2.0059
16	5	1.2365	7.0378	.4746	-.1155	3.0015	2.0059
17	1	.8117	8.3160	.4399	-.1155	3.3056	2.0451
18	3	.8168	8.3162	.4399	.1154	3.8395	2.0916
19	1	1.2502	7.0383	.4746	.1154	4.1410	2.1308
20	5	1.2502	7.0383	.4746	.1279	4.1410	2.1308
21	4	6.2675	2.6879	.7947	.3580	4.6219	2.4367
22	5	6.2675	2.6879	.7947	.3789	4.6219	2.4367
23	1	8.1584	2.0574	.9084	.3789	4.6639	2.5646
24	2	8.8533	1.8789	.9465	-.0000	4.6871	2.6679

N	EL	LUNGH.	K^2	ALFAX	ALFAZ	GAMMAX	GAMMAZ	SIGMAX	SIGMA
0	0	0.0000	0.000000	0.0000	0.0000	.0739	.2165	1.1111	.459
1	1	2.5000	0.000000	-.1848	-.5411	.0739	.2165	1.1299	.522
2	2	.4000	1.562026	7.2299	-5.3221	4.8832	3.6024	.9978	.609
3	1	.3460	0.000000	5.5403	-6.5685	4.8832	3.6024	.7695	.747
4	3	.4000	1.563791	1.4841	1.6902	.8225	.2681	.5959	.810
5	1	.5990	0.000000	.9915	1.5296	.8225	.2681	.4686	.754
6	5	0.0000	.026331	.9280	1.8577	.7720	.3573	.4686	.754
7	4	1.3100	.200000	-.0415	1.3896	.8195	.3573	.3473	.612
8	5	0.0000	.026331	-.0737	1.6057	.8225	.4361	.3473	.612
9	1	1.4770	0.000000	-1.2886	.9615	.8225	.4361	.6292	.448
10	3	.4000	.465672	-2.4640	1.4375	1.5047	.8944	.7621	.395
11	1	.5830	0.000000	-3.3412	.9160	1.5047	.8944	1.0016	.306
12	2	.4000	2.029000	3.3538	-.9165	1.5162	.8948	1.0013	.306
13	1	.3000	0.000000	2.8989	-1.1850	1.5162	.8948	.8770	.350
14	5	0.0000	.026331	2.7356	-1.1142	1.3678	.8343	.8770	.350
15	4	1.3100	.200000	.9679	-2.2071	1.5665	.8343	.4300	.566
16	5	0.0000	.026331	.9354	-2.0218	1.5164	.7229	.4300	.566
17	1	.3000	0.000000	.4805	-2.2387	1.5164	.7229	.3685	.616
18	3	.4000	1.335500	-.4940	2.2382	1.5231	.7226	.3688	.616
19	1	.3000	0.000000	-.9509	2.0214	1.5231	.7226	.4307	.566
20	5	0.0000	.026331	-.9838	2.2067	1.5740	.8339	.4307	.566
21	4	1.3100	.200000	-2.7581	1.1142	1.3733	.8339	.8788	.350
22	5	0.0000	.026331	-2.9232	1.1850	1.5229	.8945	.8788	.350
23	1	.3000	0.000000	-3.3800	.9167	1.5229	.8945	1.0033	.306
24	2	.2000	2.029000	-.0000	-.0000	.1130	.5322	1.0034	.306

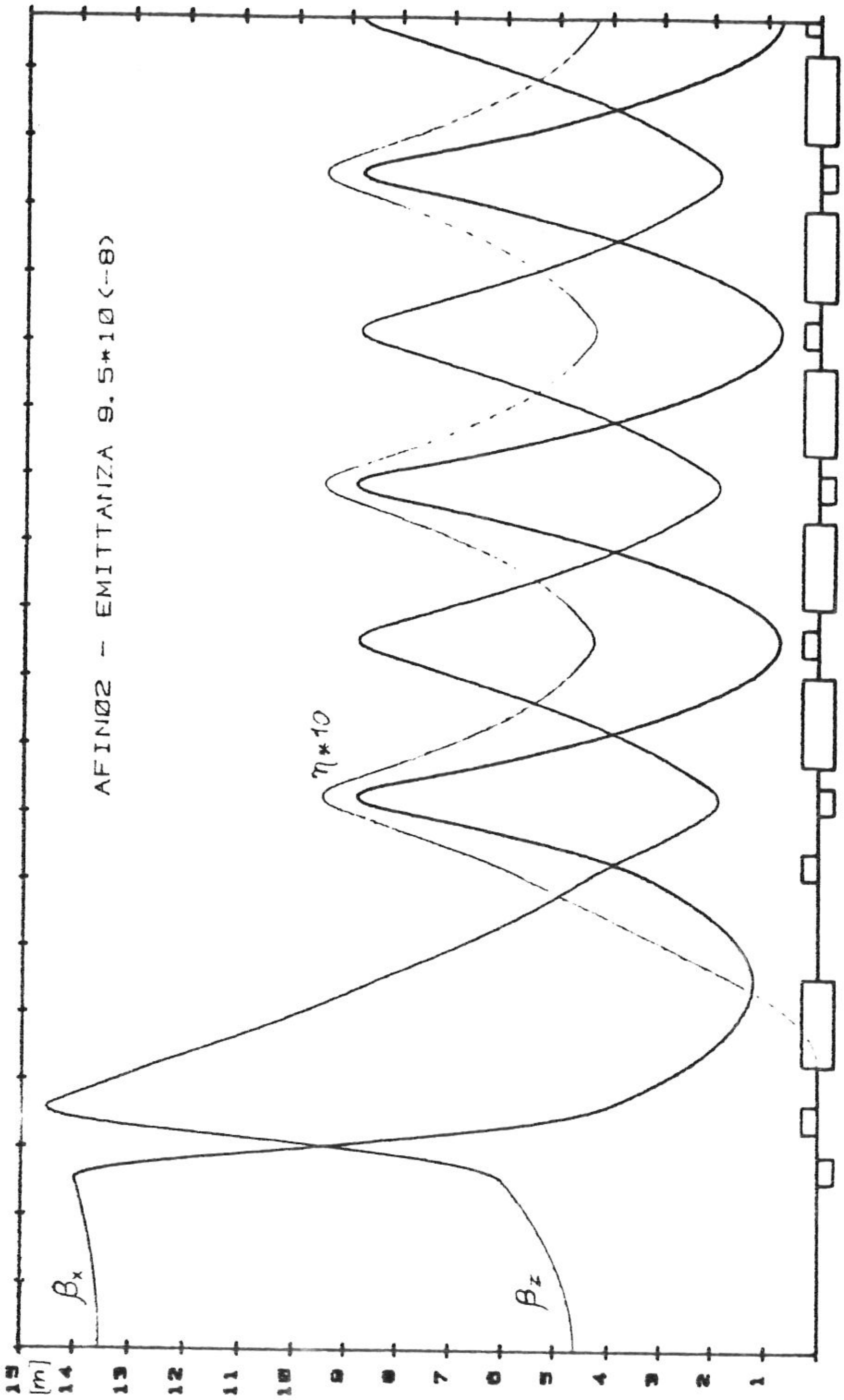

Fig. 1

LABORATORI NAZIONALI DI FRASCATI DELL'INFN

DIVISIONE MACCHINE - MEMORANDUM INTERNO

DATA	Pag 7
Gruppo e Numero	AF-2
NOME	

TITOLO

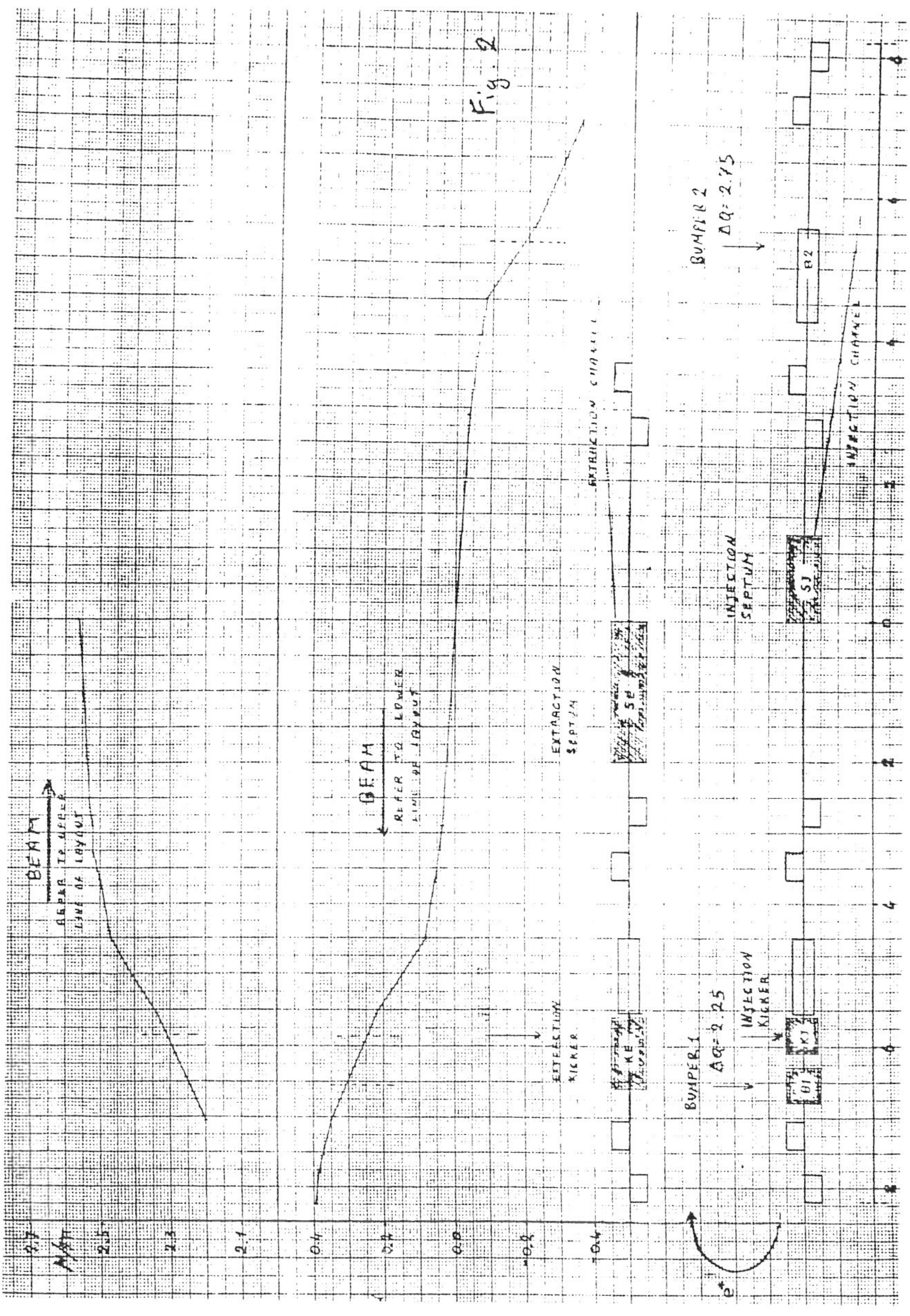

Fig. 2

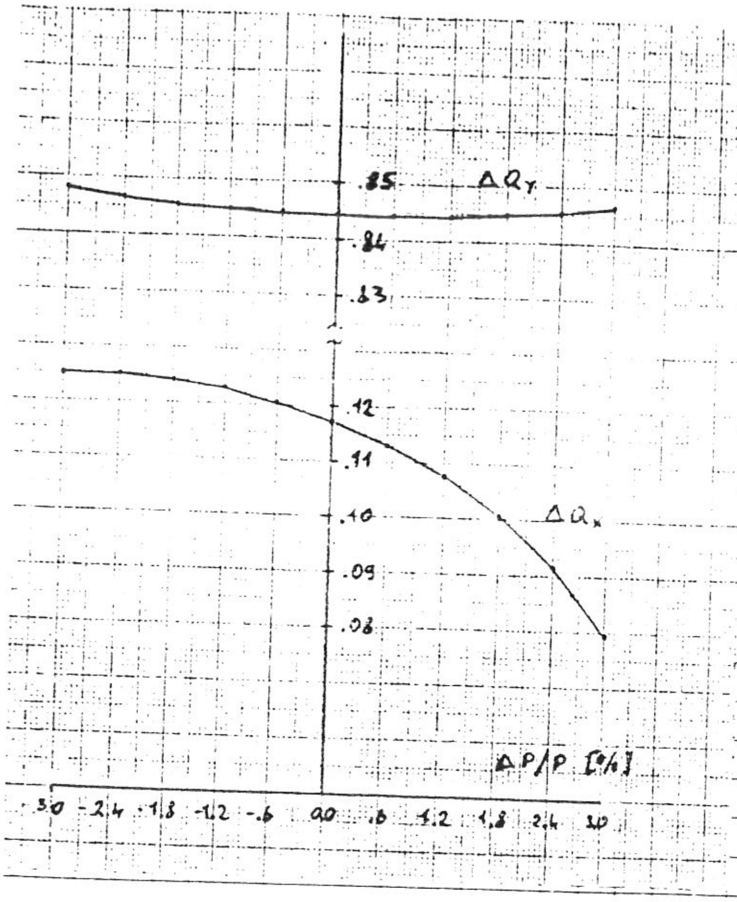

Fig. 3
Dipendenza dall' energia della parte frazionaria di Qx e Qz

Fig. 4
Variazione percentuale di β_x e β_z in funzione dell' energia

Fig. 5

Variazione di η in funzione dell' energia

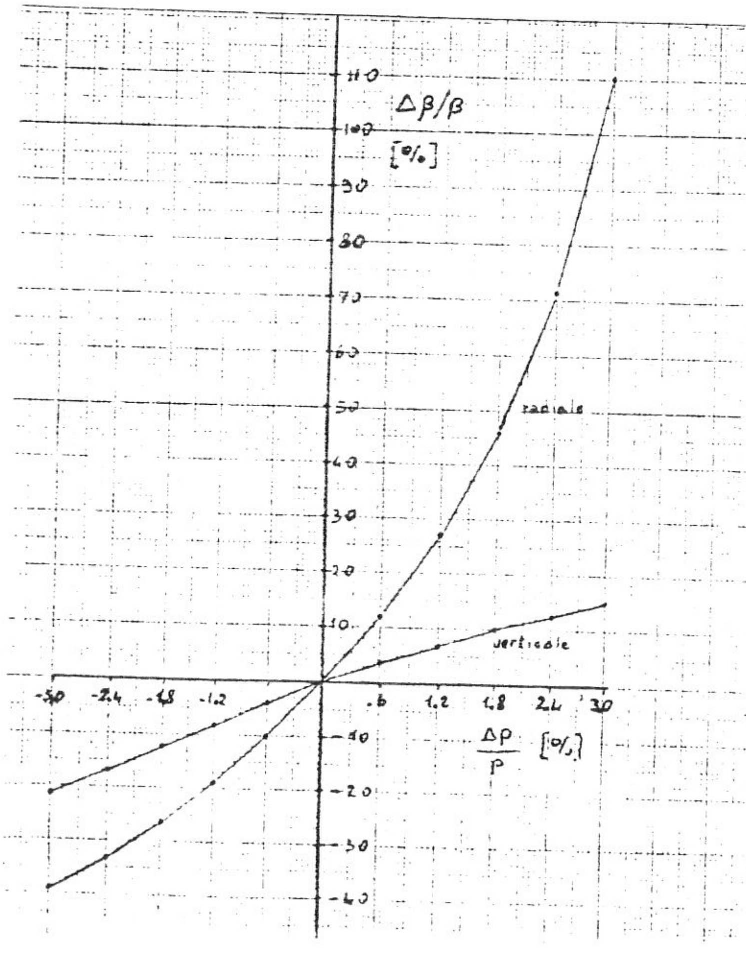

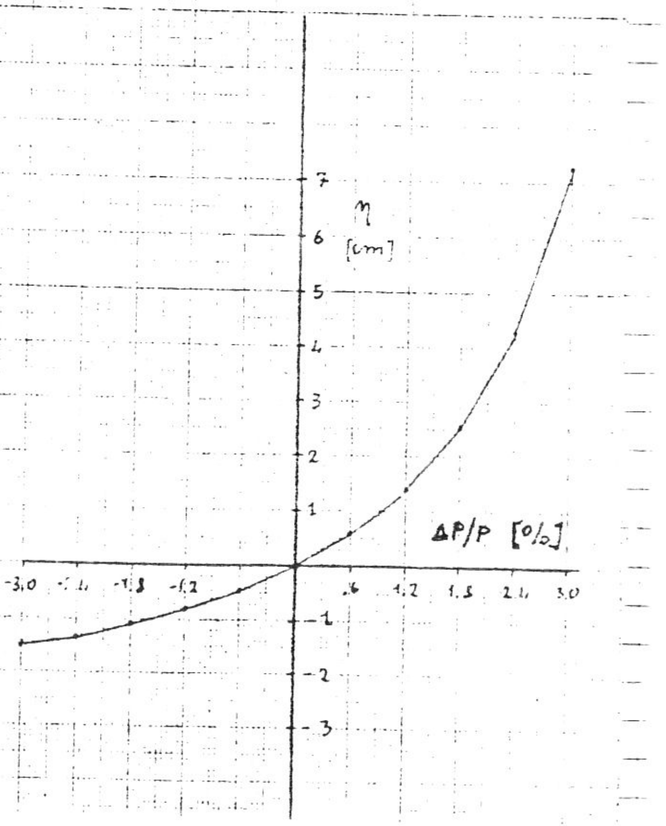

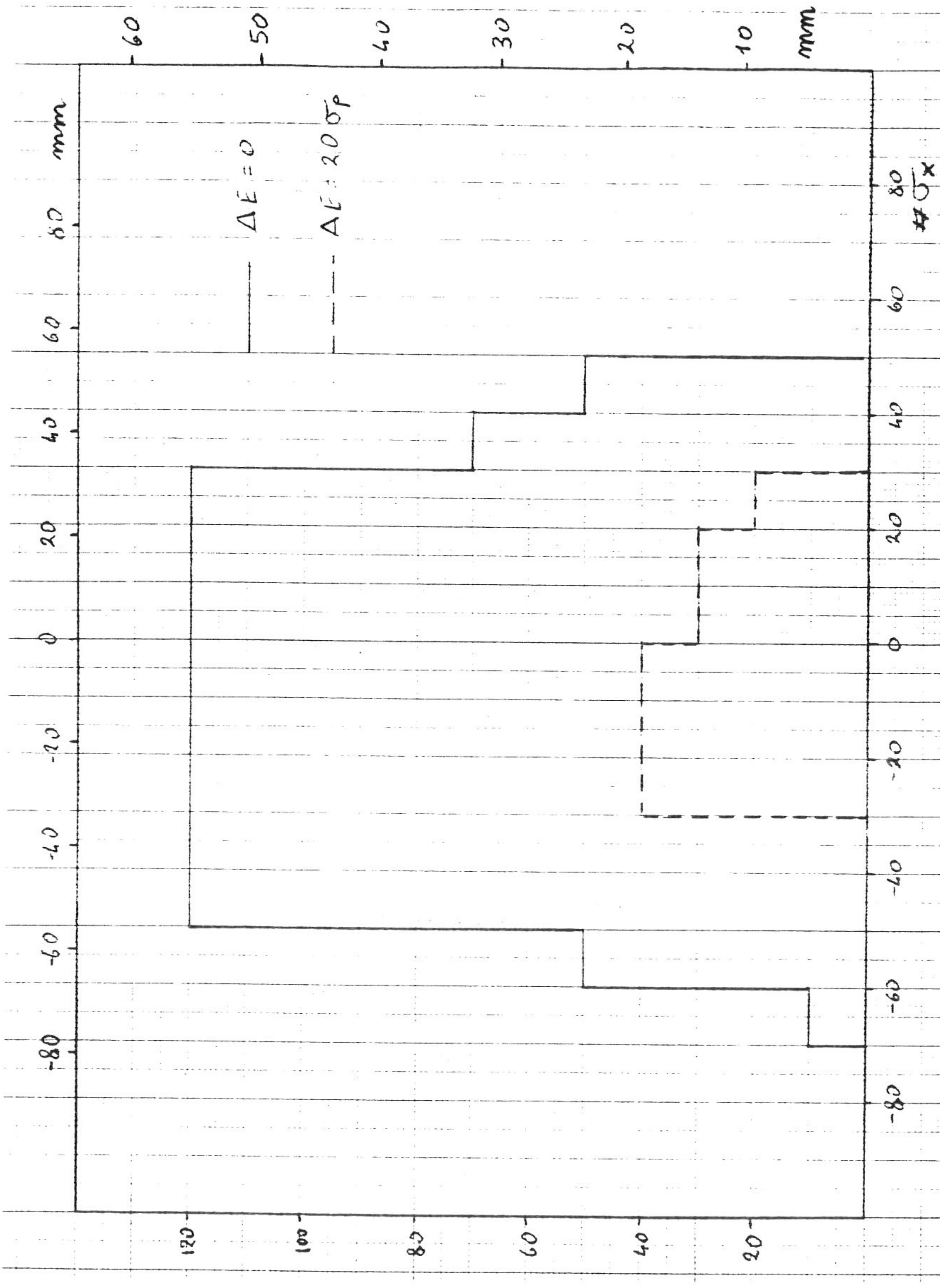

Fig.6 - Dynamical aperture at injection point